Isostructural solid-solid transition in crystalline systems with short-ranged interaction

Peter Bolhuis, Maarten Hagen, and Daan Frenkel
FOM Institute for Atomic and Molecular Physics, Kruislaan 407, 1098 SJ Amsterdam, The Netherlands
(Received 20 June 1994)

Monte Carlo simulations show that dense systems of spherical particles with a short-ranged attractive interaction can undergo a first-order transition from a dense to a more expanded solid phase with the same structure. This phase transition is analogous to the liquid-vapor transition in systems with longer-ranged attractive forces. In particular, the solid-solid transition terminates in a critical point. Numerical simulations on a square-well model indicate that a solid-solid transition will occur both in two and in three dimensions if the width of the attractive well is less than 7% of the hard-core diameter. For a hard-core Yukawa model, the transition occurs at a comparable value of the width of the attractive well. We argue that the solid-solid phase transition should be experimentally observable in mixtures of uncharged colloids and nonadsorbing polymers.

PACS number(s): 64.70.Kb, 61.20.Ja, 82.70.Dd

INTRODUCTION

Since the work of van der Waals, it is known that there is no essential distinction between a liquid and a vapor: above the critical temperature T_c, a vapor can be compressed continuously all the way to the freezing point. But below T_c, a first-order phase transition separates the dilute fluid (vapor) from the dense fluid (liquid). Yet, although the van der Waals theory becomes exact in the limit of weak, long-ranged intermolecular interactions [1], there is no fundamental reason why the liquid-vapor transition should occur in every atomic or molecular substance, nor is there any rule that forbids the existence of more than one fluid-fluid transition. Whether a given compound will have a liquid phase depends sensitively on the range of the intermolecular potential: as this range is decreased, the critical temperature approaches the triple-point temperature and when T_c drops below the latter, only a single stable fluid phase remains. This phenomenon is well known in mixtures of spherical colloidal particles and nonadsorbing polymer, where the range of the attractive part of the effective colloid-colloid interaction can be varied by changing the size of the polymer [2–6]. Experiment, theory, and simulation all suggest that when the width of the attractive well becomes less than approximately one-third of the diameter of the colloidal spheres, the colloidal "liquid" phase disappears. In fact, there is numerical evidence that in a molecular compound (C_{60}), the range of the intermolecular attraction may be sufficiently short to suppress the liquid-vapor transition [7,8].

In this paper, we consider what happens in colloidal systems with a very short-ranged attraction, where the liquid-vapor transition is absent. In Ref. [9] we presented preliminary evidence that these systems may exhibit a type of solid-solid transition that is in many ways reminiscent of the liquid-vapor transition: in particular, (i) the transition takes place between two phases that have the *same* structure, (ii) the line of (first-order) solid-solid transitions ends in a critical point, and (iii) the transition depends strongly on the range of the intermolecular attraction.

As a first approximation, we use the square-well potential to model short-ranged interactions in colloids. This model, although simple, should provide an adequate description of a wide class of uncharged colloidal particles with short-ranged attraction. The square-well model has been the subject of many theoretical and simulation studies [10,11]. In particular, the molecular dynamics studies of Young and Alder [11] on the phase diagram of a long-ranged square-well system already show the possibility of a solid-solid phase transition. However, as the authors of Ref. [11] correctly point out, the latter transition is an artifact of the square-well model and is not expected to occur in any a real system. As we shall show below, the occurrence of the solid-solid transition in systems with short-ranged potentials is not sensitive to the precise form of the potential and is therefore more likely to be experimentally observable. Additional evidence for the insensitivity of the solid-solid transition to the precise shape of the intermolecular potential comes from very recent theoretical work by Tejero *et al.* [12]. These authors predict the existence of a solid-solid transition in yet another model of particles with a short-ranged attractive potential.

An interesting question that we address in the present paper is whether or not the solid-solid transition exists in other than three dimensions. It is well known that systems with a short-ranged attraction cannot exhibit a phase transition in one dimension, but the solid-solid phase separation could occur in two-dimensional colloidal systems. Our simulations show that this is indeed the case.

The simulation results also indicate that the critical temperature of the solid-solid transition remains finite in the limit of infinitely narrow well width. We study this

limit by simulation of a lattice model and compare the results of the lattice model with that of the well-known adhesive sphere model introduced by Baxter [13].

In Sec. I we present our simulation results on the square-well model for both two and three dimensions, followed by the discussion on the infinitely narrow well-width limit. In Sec. II we discuss the application of a simple uncorrelated cell model to the square-well system. These calculations provide considerable insight into the mechanism of the phase transition.

To verify that the solid-solid transitions is not an artifact of the square-well model we also performed extensive simulations on hard-core systems with an attractive Yukawa potential. The latter model is thought to provide a fairly realistic description of the effective colloid-colloid interaction in mixtures of uncharged colloids and nonadsorbing polymer [3,5,6]. The results of the Yukawa simulations are presented in Sec. III.

I. SQUARE-WELL SYSTEMS IN TWO AND THREE DIMENSIONS

A. Solid-solid coexistence

The square-well model provides a very simple description of particles interaction through a pair potential that is harshly repulsive at distances less than a characteristic diameter σ and has an attractive interaction with a characteristic range δ outside the repulsive core. The functional form of the square-well potential is

$$v(r) = \begin{cases} \infty, & 0 \le r < \sigma \\ -\epsilon, & \sigma \le r < \sigma + \delta \\ 0, & r \ge \sigma + \delta, \end{cases} \tag{1}$$

where ϵ is the depth of the attractive well. In order to compute the phase diagram of the square-well system, we first must determine the dependence of the Helmholtz free energy of the solid on density and temperature. As the free energy of the solid cannot be measured directly in a Monte Carlo simulation, we use thermodynamic integration to relate the free energy of the square-well solid to that of a reference hard-sphere solid at the same density [14]:

$$F(\rho,\epsilon^*) = F_{\rm HS}(\rho) + \int d\epsilon^* \left(\frac{\partial F}{\partial \epsilon^*}\right)$$

$$= F_{\rm HS} + \int d\epsilon^* \frac{\langle E\rangle_{\epsilon^*}}{\epsilon^*}, \tag{2}$$

where ϵ^* is the reduced well depth ϵ/k_BT and $\langle E\rangle$ the average internal energy of the system, a quantity that *can* be measured in a Monte Carlo simulation at constant number of particles (N), volume (V), and temperature (T). The instantaneous energy is equal to the number of pairs of atoms N_p that are within the range of the potential times the depth of potential well ϵ. The dimensionless free energy per particle now is simply

$$\frac{F(\rho,\epsilon^*)}{Nk_BT} = \frac{F_{\rm HS}(\rho)}{Nk_BT} - \int d\epsilon^* \frac{\langle N_p\rangle_{\epsilon^*}}{N}. \tag{3}$$

The free energy of the three-dimensional hard-sphere solid $F_{\rm HS}$ is well known and can be accurately represented using the analytic form for the equation of state proposed by Hall [15]. In two dimensions the free energy of the hard-disk "solid" can be obtained from simulations done by Alder *et al.* [16].

The presence of a first-order phase transition in the square-well solid is signaled by the fact that the Helmholtz free energy becomes a nonconvex function of the volume. The densities of the coexisting phases can then be determined by a standard double-tangent construction.

In order to map out the phase diagram of the square-well solid over a wide range of densities and temperatures as a function of the width of the attractive well, several thousand independent simulations were required. To keep the computational costs within bounds, we chose to simulate a relatively small system. With a small system size, finite-size effects are expected, in particular, in the vicinity of a critical point. However, away from critical points finite-size effects should be so small that they will not affect the conclusions that we draw below. In what follows, we use reduced units, such that ϵ/k_B is the unit of temperature and σ, the hard-core diameter of the particles, is the unit of length.

For the two-dimensional case, the simulation parameters were as follows: All simulated systems consisted of a periodic triangular lattice of 200 disks, placed in a rectangular simulation box with side ratio $\sqrt{3}$. The densities ranged from $\rho = 0.8$, which is below the hard-disk "melting point," to $\rho = 1.154$, which is almost at close packing ($\rho_0 = 2/\sqrt{3}$). The temperature of the system was varied in the range $0 \le 1/T \le 2$, in steps of 0.1. Simulations were performed for $\delta = 0.01, 0.02, 0.03, 0.04, 0.05, 006$, and 0.07.

All simulations on the three-dimensional system were performed on a face-centered-cubic (fcc) solid consisting of 108 particles. This is presumably the stable solid structure for hard spheres [17] and for the square-well model with short-ranged attraction (i.e., only nearest-neighbor interaction). The simulation box was chosen to be cubic and periodic boundaries were applied. The densities ranged from $\rho = 0.9$, which is below the hard-sphere melting point, to $\rho = 1.414$, which is almost at close packing ($\rho_0 = \sqrt{2}$). The temperature of the system was varied over the same range as in the two-dimensional case. Simulations were performed for $\delta = 0.001$, 0.002, 0.003, 0.004, 0.005, 0.01, 0.02, 0.03, 0.04, 0.05, and 0.06. For every value of the well width δ in both the two- and the three-dimensional case, we performed some 1000 MC simulations of 20 000 cycles each.

In order to perform the double-tangent construction on the Helmholtz free energy, all simulation data were fitted to an analytic function of ρ, δ, and T. We chose to use a fit function that reproduced the correct limiting behavior at close packing. In particular, for the two-dimensional (2D) case, we used the functional form

TABLE I. Best fit coefficients c_{ijk} for Eq. (4).

		k						
i	j	0	1	2	3	4	5	6
0	0	-0.72694	0.31198	-0.25649	1.11286	-1.49782	0.69590	-0.10720
0	1	-0.03715	1.24634	5.70997	-16.67303	15.62463	-6.13765	0.87198
0	2	0.02852	0.972982	-6.07053	12.64276	-11.29891	4.52050	-0.66905
1	0	5.25367	-34.75364	101.28334	-150.72832	112.86532	-40.90991	5.71196
1	1	9.66389	0.17419	-165.09344	387.68260	-351.99452	141.41783	-20.97474
1	2	5.82891	-66.85580	245.34140	-396.61941	310.50889	-115.36343	16.28254

$$N_p(\delta, T^{-1}, x)/N = \frac{3}{2} + \frac{3}{2}\,\mathrm{erf}\left(\frac{3}{4}x - \frac{1}{2}\right) + e^{-x}\sum_{i,j,k=0}^{1,2,6} c_{ijk}\delta^i T^{-j} x^k \qquad (4)$$

and in the three-dimensional case we chose the form

$$N_p(\delta, T^{-1}, x)/N = 3 + 3\,\mathrm{erf}\left(x - \frac{3}{4}\right) + e^{-x}\sum_{i,j,k=0}^{1,2,6} c_{ijk}\delta^i T^{-j} x^k. \qquad (5)$$

The parameter x in Eqs. (4) and (5) is defined as the ratio of well width d to the distance a that characterizes the expansion of the solid from close packing: $a \equiv r_{\mathrm{NN}} - \sigma$, where r_{NN} is the average nearest-neighbor distance and σ is the hard-sphere diameter. x is simply related to the density through

$$x = \frac{\delta}{a} = \frac{\delta}{\left(\frac{\rho_0}{\rho}\right)^{\frac{1}{D}} - 1}, \qquad (6)$$

where D is the dimensionality of the system. For large x, i.e., near close packing, the functions given in Eqs. (4) and (5) go to the value of half the number of nearest neighbors per particle. The coefficients of the best fits to the numerical data are given in Tables I and II. These fits reproduce the numerical data to within the statistical error. Using the functional forms given by Eqs. (4) and (5) to represent the numerical data, we computed the free energy of the solid as a function of temperature and volume, using Eq. (3). The resulting free-energy functions were checked for a possible nonconvex dependence on the volume V. Whenever such an indication of a first-order phase transition was found, the densities of the coexisting phases were determined by equating the pressures and chemical potentials in both phases using the standard double tangent construction. The critical temperature of the solid-solid coexistence curve was estimated to be the point where the free-energy curve first developed an inflection point. Of course, this estimate is likely to depend somewhat on the system size. Moreover, the analytic form of Eqs. (4) and (5) forces the classical (mean-field) critical behavior on the solid-solid binodal. We have not attempted to study the true critical behavior of the solid-solid transition.

B. Fluid-solid coexistence

Although the solid-solid transition coexistence curves can be obtained from simulations, we have yet to demonstrate that this transition involves phases that are thermodynamically stable. In particular, the melting transition transition might preempt the solid-solid phase separation. It is therefore essential to study the fluid-solid transition as well. We computed the solid-fluid coexistence curve by means of thermodynamic integration. The Helmholtz free energy of square-well solid was calculated according to Eq. (2) using our simulation data. The free energy of the fluid phase was obtained by combining data from our simulations of a square-well fluid with the known free energy of the hard-sphere reference fluid [18]. In the two-dimensional case the fluid simulations were performed on a system consisting of 200 disks with square-well potential in a square box. The densities ranged from $\rho = 0.81$, which is below the hard-disk fluid-solid transition at $\rho = 0.87$ [19], to $\rho = 0.95$, well above the melting density. The other simulation parameters were the same as in the two-dimensional square-well solid simulation.

To simulate the fluid in three dimensions, we used a system of 108 square-well spheres in a periodic cubic box. The density was varied from $\rho = 0.9$ to $\rho = 1.0$ and the

TABLE II. Best fit coefficients c_{ijk} for Eq. (5).

		k						
i	j	0	1	2	3	4	5	6
0	0	-0.84230	-0.17552	1.09902	-2.39716	0.75281	0.22673	-0.08604
0	1	-0.09405	2.33404	12.76261	-34.81551	31.47235	-11.86920	1.59704
0	2	0.09995	1.46334	-7.59121	11.86321	-7.70867	2.09709	-0.187279
1	0	0.58991	16.75031	-66.39091	86.77000	-59.36635	20.52549	-2.76241
1	1	43.01628	-354.03802	968.06124	-1239.22030	808.64141	-259.20230	32.32189
1	2	-13.27615	87.45912	-212.72385	240.10069	-134.45590	36.047739	-3.66216

well width ranged from $\delta = 0.01$ to $\delta = 0.06$. The simulation parameters were equal to those chosen for the solid simulations. For both the 2D and 3D simulations the initial random configuration was compressed to the required density and equlibrated for 20 000 cycles before data were collected in a production run of 20 000 cycles. To calculate the fluid-solid coexistence one needs the absolute free energy of both the reference fluid and the reference solid phase. For the free energy of the hard-disk fluid we used a Padé approximation proposed by Hoover and Ree [19]. The hard-disk solid free energy was obtained from simulation data by Alder *et al.* [16]. The free energy of the hard-sphere fluid was calculated using the accurate Carnahan-Starling equation of state [18], whereas the Hall equation of state [15] was used in the solid region together with an absolute free-energy value obtained from simulations of Frenkel and Ladd [20]. Using these reference free energies and the simulated average internal energies in Eq. (2) we were able to obtain the coexistence curves for the fluid-solid transition for both the two- and three-dimensional square-well models.

C. Results

Figures 1 and 2 show the computed solid-solid and fluid-solid coexistence curves in the (ρ, T) plane for the two- and three-dimensional square-well models. We first focus on the solid-solid transition. The density gap between the dense and expanded fcc solids is wide at low temperatures and shrinks to zero when the solid-solid critical point is approached. Because of the analogy with liquid-vapor coexistence, one would expect that the solid-solid critical point should be of the 2D and the 3D Ising universality class.

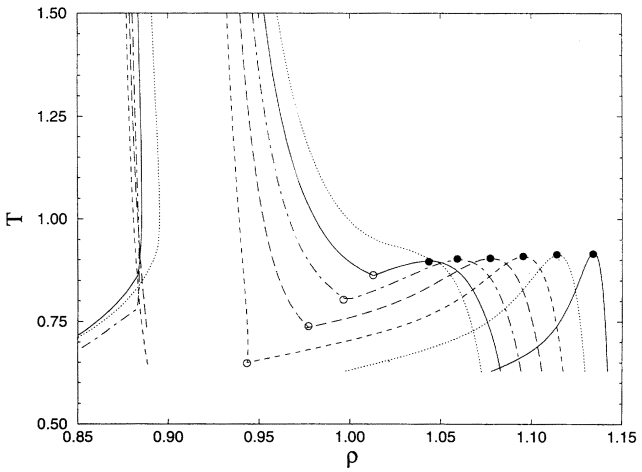

FIG. 1. Simulated (T, ρ) phase diagrams for triangular lattice of 200 square-well particles in two dimensions. Starting with the coexistence curve on the right, from right to left the curves correspond to the well widths $\delta/\sigma = 0.01, 0.02, 0.03, 0.04, 0.05, 0.06$, and 0.07. Solid-fluid coexistence curves are shown for all systems with $\delta/\sigma \geq 0.03$. The critical points are indicated by filled circles, the triple points by open circles.

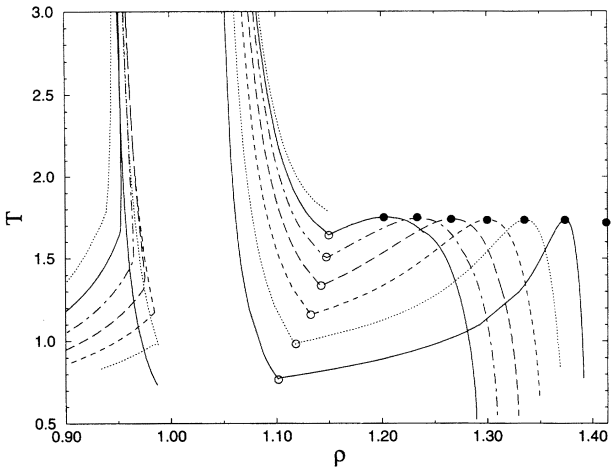

FIG. 2. Simulated (T, ρ) phase diagrams for the fcc structure of 108 square-well particles. Starting with the coexistence curve on the right, from right to left the curves correspond to the well widths $\delta/\sigma = 0.01, 0.02, 0.03, 0.04, 0.05$, and 0.06. The upper dashed fluid-solid coexistence curve refers to a well width of $\delta/\sigma = 0.07$ and shows that the solid-solid transition has become metastable at this point. The critical points are indicated by filled circles, the triple points by open circles. The critical point at $\rho = \sqrt{2}$, corresponding to $\delta/\sigma = 0$, was computed using the lattice model described in Sec. I D.

The coexistence curves are asymmetric, especially in the limit $\delta \to 0$. In this limit, the reduced critical temperature T_c goes to a finite limiting value of approximately 1.7 for $D = 3$ and 0.92 for $D = 2$. As we shall argue below, the phase behavior in this limit can be investigated by studying a peculiar lattice model.

As can be seen in Figs. 1 and 2, the critical temperature depends only weakly on δ. In contrast, the solid-solid coexistence region shifts to lower densities as the well width is increased. This effect can easily be understood by noting that a dense square-well solid can be expanded at virtually no cost in potential energy, up to the point where the nearest-neighbor separation is $1+\delta$, that is, $a = \delta$. It is only when the solid is expanded beyond this limit that the potential energy increases steeply and a transition to the expanded solid may occur. Hence the larger δ, the lower the density where the phase transition will take place.

The fluid-solid coexistence curves are also dependent on δ. For small δ the width of the coexistence density gap between fluid and solid remains effectively constant as a function of temperature, although as a whole it shifts to a higher density as the temperature is lowered. If δ is increased, the density gap widens at low temperature.

The point where the coexistence curves cross the solid-solid binodals is the triple point T_p, where the three phases (fluid, solid I, and solid II) are in equilibrium. At temperatures below the triple point the high-density solid is in equilibrium with a dilute gas. When δ becomes larger, the triple point shifts to higher temperatures and densities, until it reaches the critical temperature. At

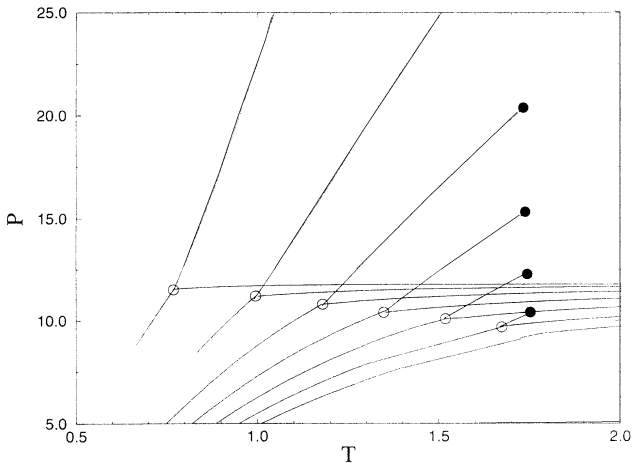

FIG. 3. Simulated phase diagrams of the three-dimensional square-well system plotted in the (P,T) plane. The solid-solid transition lines run from the triple point, denoted by an open circle to the critical point, marked by a filled circle. The lower curves are the melting lines of the square-well system. From left to right the diagrams correspond to $\delta/\sigma = 0.01, 0.02, 0.03, 0.04, 0.05$, and 0.06. Note that this phase diagram is almost a mirror image of the fluid-gas (P,T) phase diagram. Also note that the slope of the solid-solid transition has to be positive.

that point the solid-solid transition disappears because for larger values of δ it is preempted by the melting transition. Both in two and three dimensions, this happens when $\delta > 0.06$.

It is instructive to draw the phase diagram in the (P,T) plane. In Fig. 3 the phase diagrams for the three-dimensional square-well system are shown in the (P,T) plane. The solid-solid transition lines run from the triple point to the critical point and lie above the melting lines of the square-well system. The phase diagram for short-ranged attractive potential is the mirror image of the usual (P,T) phase diagram for longer ranged potentials in which the liquid-gas transition is present. Note that the slope of the solid-solid transition line cannot be negative because the critical temperature has to be higher than the triple point temperature.

D. High density limit

The simulations discussed above seem to indicate that there is a solid-solid transition even in the limit where $\delta \to 0$. At first sight this seems surprising because one would not expect an infinitely narrow potential well to affect the phase behavior at finite temperature. However, at close packing, even an infinitely narrow potential will give a finite contribution to the potential energy. Surprisingly, it turns out that it is possible to perform simulations of the phase behavior in the limit $\delta \to 0$. To see how this can be achieved, it is convenient to consider first the more general case that δ is finite. In the dense crystalline solid, any given particle i is constrained to move in the vicinity of its lattice site, i.e., its average position $\mathbf{r}_i^0$. In that case, we can reexpress the potential energy as a function of the displacement Δ_i of the particles, from their respective lattice sites: $\mathbf{\Delta}_i \equiv \mathbf{r}_i - \mathbf{r}_i^0$. The potential energy of a pair of particles can then be written as

$$v(\mathbf{r}_{ij}) = v(|\mathbf{r}_i^0 - \mathbf{r}_j^0 + \mathbf{\Delta}_i - \mathbf{\Delta}_j|), \tag{7}$$

where we have used the obvious notation $\mathbf{r}_{ij} \equiv \mathbf{r}_i - \mathbf{r}_j$. For nearest neighbors, $|\mathbf{r}_i^0 - \mathbf{r}_j^0| = \sigma$ at close packing. At lower densities, $|\mathbf{r}_i^0 - \mathbf{r}_j^0| = \sigma + a$, where a was defined in Eq. (6). The potential energy of a pair of square-well particles is a function of $z_{ij} \equiv (|\mathbf{r}_{ij}| - \sigma)/\delta$. We can now express $\mathbf{r}_{ij}$ in terms of $\mathbf{\Delta}_i$ and $\mathbf{\Delta}_j$. This yields the following result for z_{ij}:

$$z_{ij} = \frac{\sqrt{\sigma^2 + 2\sigma(a + \hat{\mathbf{r}}_{ij} \cdot \mathbf{\Delta}_{ij}) + a^2 + \Delta_{ij}^2 + 2a\hat{\mathbf{r}}_{ij} \cdot \mathbf{\Delta}_{ij}} - \sigma}{\delta}, \tag{8}$$

where $\hat{\mathbf{r}}_{ij}$ is a unit vector in the direction of $\mathbf{r}_{ij}^0$ and $\mathbf{\Delta}_{ij} = \mathbf{\Delta}_i - \mathbf{\Delta}_j$. In the limit $\delta/\sigma \to 0$, z_{ij} takes on a very simple form

$$\lim_{\delta/\sigma \to 0} z_{ij} = \frac{a + \hat{\mathbf{r}}_{ij} \cdot \mathbf{\Delta}_{ij}}{\delta}. \tag{9}$$

In this limit, the square-well model is equivalent to a lattice model, with a fixed but arbitrary lattice spacing as shown in Fig. 4. The state at every lattice point i is characterized by a scaled displacement vector $\mathbf{v}_i \equiv \mathbf{\Delta}_i/\delta$. Note that a finite $\mathbf{v}_i$ corresponds to an infinitesimal real displacement $\mathbf{v}_i\delta$. The nearest-neighbor interaction is a function of $a/\delta + \mathbf{v}_i \cdot \hat{\mathbf{r}}_{ij}$. Clearly, the density in the original square-well model now only enters in the problem through the parameter a/δ. We can now perform Monte Carlo simulations on this lattice model by moving a randomly selected atom i from its initial scaled displacement $\mathbf{v}_i$ to the trial displacement $\mathbf{v}_i'$ in such a way that microscopic reversibility is satisfied. Knowledge of the new scaled displacement of atom i is sufficient to compute the change in potential energy associated with the trial move, using Eqs. (7)–(9) above. We now use the conventional Metropolis rule to accept or reject the trial move. By combining the results of a series of simulations for a range of values of δ/a and a range of temperatures (twenty temperatures and thirty δ/a values for every temperature) with the hard-sphere equation of state near close packing [21], we can compute the free energy of this model system as a function of temperature and volume by thermodynamic integration and construct the solid-solid phase diagram in the limit $\delta/\sigma = 0$. In the (ρ,T) plane, the binodal would simply be a vertical line segment at

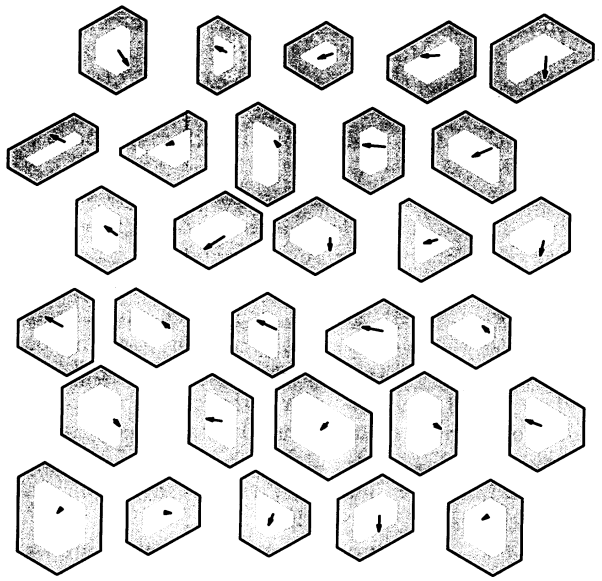

FIG. 4. Schematically drawn scaled configuration of the (2D) square-well solid in the limit $\delta/\sigma \to 0$. The lines of the hexagons give the momentary boundary of the cell to which a particle is confined. All the cell are scaled up to finite size, as the cells are infinitely small in the limit $\delta/\sigma \to 0$. The cell boundaries will change position if the nearest neighbors move. The arrows give the particle displacement from their original lattice positions. In the shaded area the particles are within the interaction range of their neighbors.

close packing ending in a critical point. It is more convenient to plot the binodal as a function of δ/a. In Fig. 5 the solid-solid binodal is plotted in the $((\delta/a), T)$ plane. As can be seen from the figure, the critical temperature is indeed finite. Moreover, the binodal becomes quite symmetric in this representation compared to Fig. 2.

It is interesting to consider the square-well solid at *finite* δ/σ in terms of the lattice model described above. As can be seen from Eqs. (7) and (8), the potential energy now is a function not only of a/δ and $\mathbf{\Delta}_i/\delta$, but also of δ/σ. If the free energy of the system is an analytic function of δ/σ, we could expand in powers of it around the limit $\delta/\sigma = 0$. However, the solid-solid transition only occurs for $\delta/\sigma \leq 0.06$. Hence δ/σ is always a small parameter. It is therefore likely that the phase diagram of the square-well model, when plotted as a function of δ/a, differs only little from the behavior in the limit $\delta \to 0$. As can be seen from Fig. 5 this is indeed the case.

It is interesting to point out the relation between the square-well model in the limit $\delta/\sigma = 0$ and the adhesive hard-sphere model proposed by Baxter [13]. The adhesive hard-sphere model is obtained from the square-well model by considering the limit $\delta/\sigma \to 0, \epsilon \to \infty$ such that $\epsilon/kT = -\ln[\sigma/(12\delta\tau)]$. This limiting procedure results in a model that has a finite second virial coefficient at finite temperature. Usually, the ratio of the second virial coefficient of the adhesive hard-sphere to that of "nonsticky" hard spheres is used to relate the parameter τ to observable quantities:

$$B_2^{\mathrm{AHS}}/B_2^{\mathrm{HS}} = 1 - \frac{1}{4\tau}. \tag{10}$$

The adhesive-hard-sphere system has been studied extensively both theoretically [22–24] and numerically [25,26]. In particular, the liquid-vapor critical point of this model has been predicted to occur at $\tau \approx 0.097$ [22]. However, if we identify the adhesive hard-sphere model with the square-well model in the limit $\delta/\sigma \to 0$, then the present simulations show that this model already has a solid-solid transition for $\tau = O(\ln(\sigma/\delta))$, i.e., for $\tau \to \infty$. At all finite temperatures (finite τ) the only stable phases are the close-packed solid and the infinitely dilute gas. Hence all other phases of the adhesive hard-sphere model are, at best, metastable. In fact, Stell [27] has already indicated that the monodisperse adhesive hard-sphere model is pathological because the 12th virial coefficient diverges. This divergence could be removed by introducing a slight size polydispersity into the model. Such polydispersity would also affect the solid-solid transition. In fact, a rough estimate of the phase-diagram suggests that in that case, the solid-fluid transition occurs at finite τ and hence

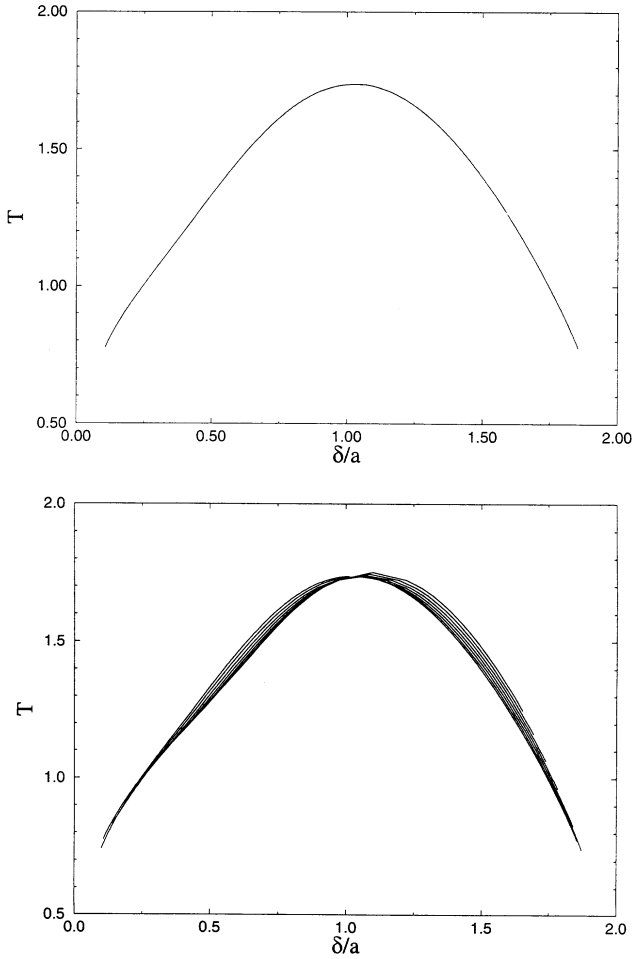

FIG. 5. Solid-solid coexistence curves in the $(\delta/a, T)$ plane (see text). The top figure shows the binodal in the limit $\delta/\sigma = 0$, while the bottom figure shows that all the scaled binodals for finite $\delta/\sigma < 0.07$ very nearly coincide with the binodal for $\delta/\sigma = 0$.

the phase diagram of the slightly polydisperse adhesive hard-sphere model is nontrivial.

II. CELL MODEL CALCULATIONS

To gain a better intuitive understanding of the solid-solid transition in the square-well model, it is instructive to compare the simulation results with a simple theoretical approach, viz., the uncorrelated cell model. The cell model is based on the idea that an atom in a solid is essentially confined to the "cell" formed by its nearest neighbors [28]. In the uncorrelated, single occupancy version of the cell model [29,30] the configurational part of the partition function of an N-particle system is approximated by

$$Q = \int dr^N e^{-\beta U(r^N)} \approx N! \left(\int dr e^{-\beta U(r, r^{\mathrm{NN}})/2} \right)^N , \quad (11)$$

where $U(r^N)$ is the potential energy of the system and $U(r, r^{\mathrm{NN}})$ is the potential energy of an atom and its nearest neighbors. Here it is assumed that a cell can contain at most one particle and that all correlations between cells can be ignored. If one further assumes that every particle moves independently in a regular fixed polyhedron formed by its neighbors fixed at their lattice positions, the second integral of Eq. (11) can be easily evaluated.

We use the square-well model to describe the short-ranged attractive interaction. Because the square-well potential is a step function, the cell volume can be divided into different regions characterized by the number of neighbors within the range of its attractive well. The partition function can now be expressed in terms of cell volume fractions α_k in which the particle intracts with k particles simultaneously

$$\frac{Q(x, \epsilon^*)}{N!} = \left(V_c \sum_{k=0}^{m} e^{k\epsilon^*/2} \alpha_k(x) \right)^N , \quad (12)$$

where $x = \delta/a$ is the parameter defined in Eq. (6), m is the maximum number of neighbors, and V_c is the volume of the cell. This volume depends on the dimensionality and the crystal structure. For a three-dimensional fcc structure the cell is a dodecahedron with a volume $V_c = a^3/\sqrt{2}$, where a, the radius of the cell, is defined as before $a \equiv r_{\mathrm{NN}} - \sigma$. In a two-dimensional triangular lattice $V_c = 2\sqrt{3}a^2$.

The Helmholtz free energy of the solid is given by the logarithm of the partition function

$$\frac{\beta F_{SW}(x, \epsilon^*)}{N} = \frac{-\ln Z(x, \epsilon^*)}{N} = -\ln \Lambda^3 V_d - \ln \left(\sum_{k=0}^{m} e^{k\epsilon^*/2} \alpha_k(x) \right). \quad (13)$$

The first term can be interpreted as the entropy of an ideal lattice gas, while the second term is the contribution due to the attractive interactions. Figure 6 shows for the triangular and fcc crystal structures the cell volume fraction α_k as a function of x. For sufficiently short-ranged potentials, the solid can be expanded to a density where a is much larger than the width of the attractive well δ. In that case, a given particle can only have a few neighbors within the range of its attractive well. When the density is increased the particle interacts with more neighbors. At $\delta/a = 1$ the particle has exactly half the number of neighbors within the potential range. Once the density is so high that $\delta/a > 2$, then every particle interacts with all its nearest neighbors simultaneously. This behavior leads to a fairly abrupt lowering of the potential energy of the system. At low temperatures, this decrease of the energy on compression will outweigh the loss of entropy that is caused by the decrease of the free volume V_d. The Helmholtz free energy F will then exhibit an inflection point and a first-order transition to a "collapsed" solid will result.

By application of a double tangent construction we can compute the coexisting densities as a function of temper-

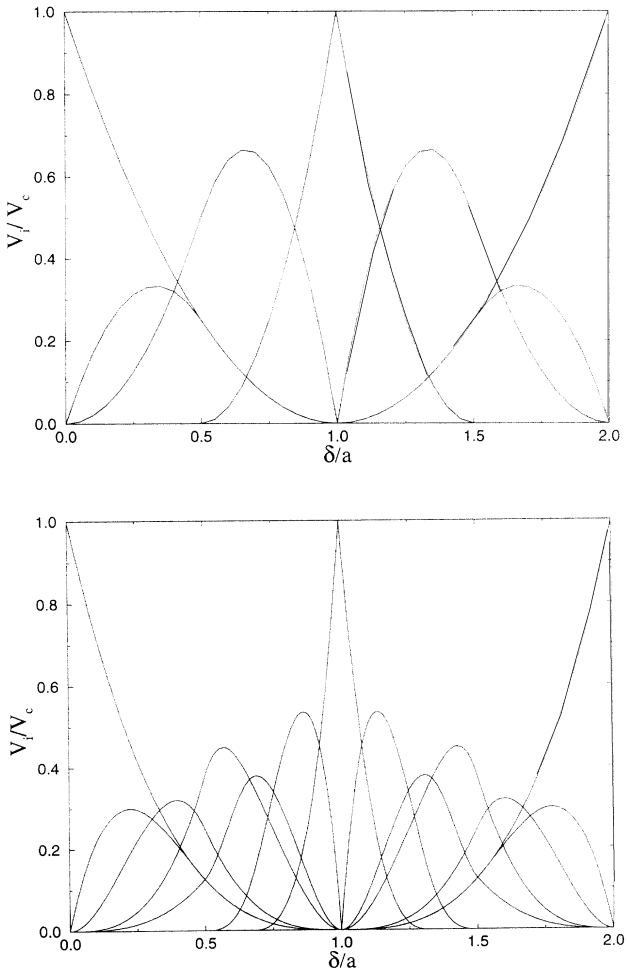

FIG. 6. Uncorrelated cell model calculation of the fraction of cell volume where the central particle interacts with k neighbors as a function of δ/a. Top figure: two-dimensional hexagonal lattice. The curves represent, from left to right, $k = 0, 1, ..., 6$. Bottom figure: three-dimensional fcc structure. From left to right the curves are for $k = 0, 1, ..., 12$.

ature. Figure 7 shows the coexistence curves in the temperature density plane for different values of the attractive well depth δ. Indeed the cell model predicts a phase separation at high density and small well width δ. The coexistence gap becomes larger when the temperature is lowered. A spurious feature of this simple cell model is that it does not predict a finite critical temperature. This stems from the fact that in the cell model there is always a discontinuity in the pressure and chemical potential that leads to a phase transition at all temperatures. The discontinuity originates from the sharp change in the volume fraction α at $a = \delta$ (see Fig. 6) in the uncorrelated cell model approximation. As the discontinuity of the pressure always takes place at a density where $\delta = a$, a very simple expression for the critical density follows

$$\rho_c = \rho_0 \left(\frac{\delta}{\sigma} + 1 \right)^{-D}, \tag{14}$$

where ρ_0 denotes the density of the solid at regular close packing.

As can be seen in Fig. 8, the dependence of the critical density on δ obtained from the simulations is described remarkably well by Eq. (14), despite the fact that the finite critical temperature is not predicted by the cell model calculations. When all correlations are taken into account, the discontinuities in the free energy derivatives should disappear and a finite critical temperature will result. Of course, more sophisticated cell model and cell cluster theories that deal with the correlations exists [21,31], but are not neccessary for our purpose. In a recent paper, Daanoun *et al.* [32] used a van der Waals–like approximation to compute the phase diagram of a square-well system. Although this approach also ignores all correlation effects, these theoretical calculations repoduce the essential features of our simulation data. Even better agreement has been found in recent density-functional theory calculations by Likos *et al.* [33].

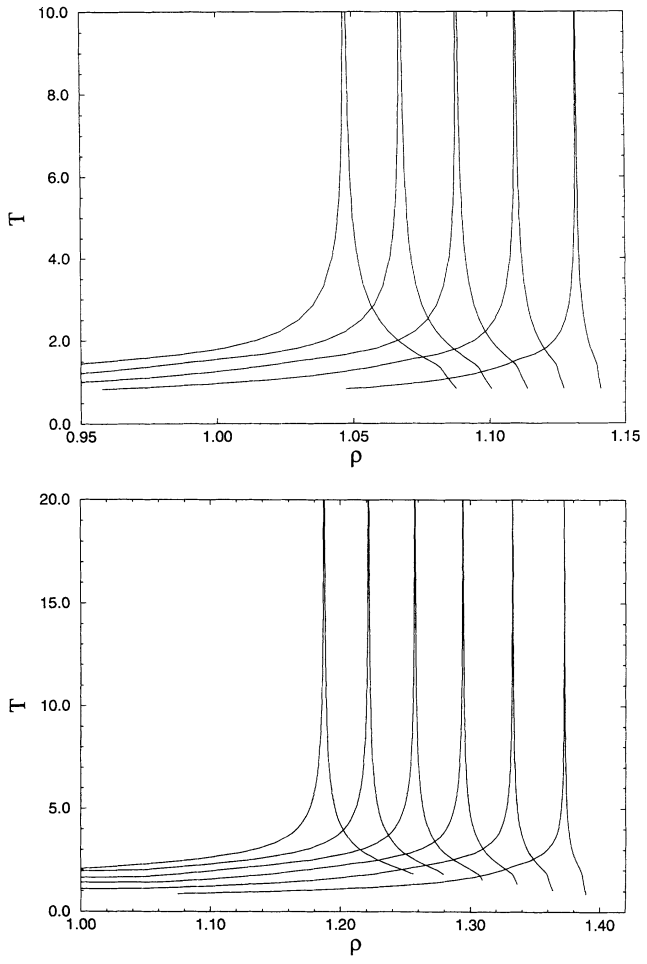

FIG. 7. Phase diagrams in the (T, ρ) plane for the square-well potential in the uncorrelated cell model approximation. Top figure: coexistence curves for a two-dimensional hexagonal lattice. From right to left $\delta/\sigma = 0.01, 0.02, 0.03, 0.04$, and 0.05. Bottom figure: coexistence curves for a three-dimensional fcc lattice. From right to left $\delta/\sigma = 0.01, 0.02, 0.03, 0.04, 0.05$, and 0.06. In both figures no critical temperature is obtained due to discontinuities in the derivatives of the cell model free energy.

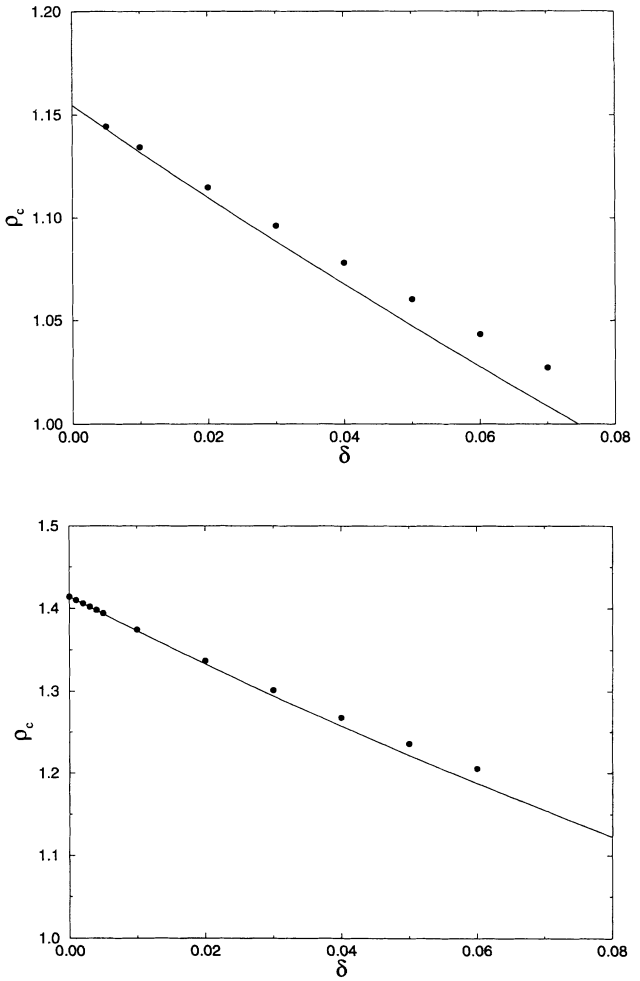

FIG. 8. Solid-solid critical density of square-well systems, as a function of the well width δ. The circles denote the simulation results, while the solid curve denotes the prediction of the uncorrelated cell model. The upper figure refers to two dimensions, while the lower figure shows the three-dimensional case.

III. YUKAWA POTENTIAL

The square-well potential is often used as a crude approximation to the effective intermolecular potential in colloid-polymer mixtures. A better approximation for the colloid-colloid interaction in such systems is the hard-core attractive Yukawa potential, given by

$$v(r) = \begin{cases} \infty, & 0 \leq r < \sigma \\ -\epsilon \left(\frac{\sigma}{r}\right) \exp\left[\kappa\sigma(1 - r/\sigma)\right], & r > \sigma, \end{cases} \tag{15}$$

where ϵ is the well depth and κ^{-1} is a measure for the range of the attractive part of the potential [5,6,4,3]. The phase diagram of the hard-core attractive Yukawa fluid was investigated recently by Hagen and Frenkel [34]. To see if the solid-solid transition survives in the case of a Yukawa potential, we did simulations on a 108 particle fcc crystal for $\kappa = 15, 20, 25, 30, 35, 40, 45$, and 50 and in the high-density limit for $\kappa \to \infty$. The densities ranged from 1.1 to 1.38. The temperatures, in reduced units of ϵ/k_B, were varied in the same range as in the square-well case, $0 \leq T^{-1} \leq 2$, in steps of 0.1. For every value of ρ, T, and κ we performed some 10 000 Monte Carlo cycles to equilibrate and the same amount to collect data. The average internal energy was fitted to a polynomial in $\kappa^{-1}, 1/T$, and $\kappa^{-1}(\rho_0/\rho - 1)^{-1}$. It was not neccesary to use the more complicated functional form given in Eq. (4) because the energies varied much more smoothly with density than in the square-well model. The Helmholtz free energy of the Yukawa solid was obtained by thermodynamic integration starting with the hard-sphere free energy [cf. Eq. (2)] and the coexistence densities as a function of temperature were calculated by applying the double tangent construction.

As in the case of the square-well model it is essential to know the position of the fluid-solid coexistence region to determine the range of densities where a solid-solid transition can take place. We estimated the location of the melting curve by first-order perturbation theory. In Ref. [34] it is shown that first-order perturbation provides quite accurate estimates of the melting curve of the hard-core attractive Yukawa system.

The Helmholtz free energy of the Yukawa system can be approximated by

$$F(\rho) = F_{\rm HS}(\rho) + \langle E_{\rm Yuk}\rangle_{\rm HS}\,, \tag{16}$$

where $\langle E_{\rm Yuk}\rangle_{\rm HS}$ is the average value of the attractive part of the Yukawa potential, computed in the hard-sphere reference system. From this equation it is possible to derive the fluid-solid coexistence by application of the double tangent construction. Simulations on a 108 particle hard-sphere fluid and hard-sphere fcc crystal were used to compute $\langle E_{\rm Yuk}\rangle_{\rm HS}$ for $\kappa = 25$ and $\kappa = 33$.

The resulting phase diagrams for $\kappa = 25$, 33, 40, 50, 67, 100, and 200 are presented in Fig. 9. The solid-solid transition is found to occur for $\kappa > 25$. For values $\kappa > 33$ the fluid-solid coexistence region will shift down, which results in a larger solid-solid two phase region. The phase diagrams of the Yukawa solid exhibit the same overall features as those of the square-well system. The solid-solid density gap is wide at low temperatures and shrinks when

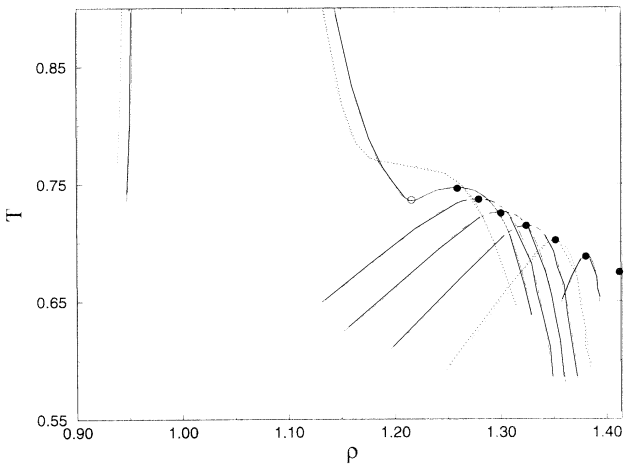

FIG. 9. Simulated (T, ρ) phase diagrams for the 108 particle fcc crystal structure with a Yukawa potential. Starting with the coexistence curve on the right, from right to left the curves correspond to $\kappa = 200, 100, 67, 50, 40, 33$, and 25. The critical points are indicated by filled circles, the triple points by open circles. The critical point at $\rho = \sqrt{2}$, corresponding to $\delta/\sigma = 0$, was computed using the lattice model described in Sec. I D. The fluid-solid coexistence was calculated only for the last two values. For higher κ values, we should expect to see the range of stability of the solid-solid coexistence line increase until, in the limit $\kappa \to \infty$, it will extend down to $T = 0$.

the critical point is reached. The critical density shifts to higher values when κ is increased, i.e., when the range of the attractive potential is shortened. However, in contrast to the square-well system the critical temperature is now clearly dependent on the potential range. The critical temperature has a value of 0.67 in the limit $1/\kappa\sigma = 0$. This was verified by direct simulations in this limit, using the technique described in Sec. I D. This critical temperature is somewhat lower than for the three-dimensional square-well solid. The reason is that the Yukawa potential is smoother than a square well. This results in an inflection point in the free-energy curve at lower temperatures. This in turn will cause all the coexistence curves to shift to lower temperature than those found in the square-well case.

The value of $\kappa = 25$, where the solid-solid transition starts to occur, corresponds to an average well width of $\kappa^{-1} = 0.04$. Although one cannot directly compare the width of a square well and a Yukawa potential, the characteristic well widths are of comparable magnitude.

CONCLUSION

Simple solids with a short-ranged atractive pair potential can exhibit phase separation in a expanded solid and a more dense solid. This isostructural first-order solid-solid transition is reminiscent of the the liquid-vapor transition. The transition takes place between two phases of the same structure, the coexistence curve ends in a

critical point, and the location of the coexistence curves depends strongly on the interaction range. The simulations on the square-well model show that the solid-solid transition takes place both in two and three dimensions for potential well widths $\delta/\sigma < 0.07$. The analogy with liquid-vapor phase separation suggests that the solid-solid critical point should be of the 2D and the 3D Ising universality class, although this still remains to be established. The critical density depends on the well width δ and is well predicted by the uncorrelated cell model. In contrast, the critical temperature hardly changes with δ. The critical temperature is finite for $\delta \to 0$. This has been confirmed by direct simulations in this limit. Comparison of the adhesive sphere model theories with the simulations in the limit $\delta \to 0$ shows that the solid-solid transition already occurs for $\tau \to \infty$, where τ plays the role of temperature in the adhesive sphere model. This implies that at finite τ the only stable phases are the close-packed solid and the infinite dilute gas. All other phases are, at best, metastable. This pathological behavior is thougth to be a consequence of the monodispersity of the system. We expect that introducing a slight size polydispersity will cause the solid-solid transition to occur at finite τ.

The results for the solid-solid transition in Yukawa systems are comparable to those for the square-well model. The solid-solid transition occurs for $\kappa\sigma > 25$, i.e., a potential well width narrower than 0.04σ. The major difference with the square-well results is that the critical temperature depends more strongly on κ.

It should be noted that isostructural solid-solid transitions are known to occur in dense Cs and Ce [35]. However, in this case the intermolecular potential is too long ranged to induce the mechanism described above and the transition is believed to be due to the *softness* of the intermolecular potential associated with a pressure-induced change in the electronic state of the metal ions. In fact, theoretical work of Stell and Hemmer [36] and simulations of Alder and Young [37] indicate that such softness may indeed result in solid-solid transition. We stress that the solid-solid transition discussed in the present paper is different because it is not related to a pressure-induced change in the effective size of the particles.

An obvious question is whether the isostructural solid-solid phase transition due to short-ranged attraction, which we report here, can occur in real systems. We believe that such a transition can be observed in uncharged colloids with a short-ranged attraction. Such systems can be made, for instance, by adding nonadsorbing polymer to a suspension of hard-sphere colloids (for a review, see, e.g., Ref. [4]). The polymers induce an effective attractive force between the colloidal spheres. The range of this attraction is directly related to the radius of gyration of the polymer. Hence a colloidal crystal to which a polymer with a radius of gyration less than 7% of the radius of the colloidal spheres has been added should exhibit the solid-solid phase behavior of the models discussed in this paper.

ACKNOWLEDGMENTS

The work of the FOM Institute is part of the research program of the Foundation for Fundamental Research of Matter (FOM) and is made possible by financial support from the Netherlands Organization for Scientific Research (NWO). We gratefully acknowledge discussions with Henk Lekkerkerker. We thank M. Baus for sending us copies of Refs. [12] and [32] and C.N. Likos for sending us a copy of Ref. [33] prior to publication.

[1] P.C. Hemmer and J.L. Lebowitz, in *Critical Phenomena and Phase Transitions 5b*, edited by C. Domb and M. Green (Academic, New York, 1976).
[2] A.P. Gast, C.K. Hall, and W.B. Russel, J. Colloid Interface Sci. **96**, 251 (1983).
[3] S. Asakura and F. Oosawa, J. Chem. Phys. **22**, 1255 (1954).
[4] P.N. Pusey, in *Liquids, Freezing and Glass Transition*, edited by J.P. Hansen, D. Levesque, and J. Zinn-Justin (North-Holland, Amsterdam, 1991), p. 763.
[5] E.J. Meijer and D. Frenkel, Phys. Rev. Lett. **67**, 1110 (1991).
[6] E.J. Meijer and D. Frenkel, J. Chem Phys. **100**, 6873 (1994).
[7] M.H.J. Hagen, E.J. Meijer, G.C.A.M. Mooij, D. Frenkel, and H.N.W. Lekkerkerker, Nature **365**, 425 (1993).
[8] L. Mederos and G. Navascués, Phys. Rev. B **50**, 1301 (1994).
[9] P. Bolhuis and D. Frenkel, Phys. Rev. Lett. **72**, 2211 (1994).
[10] J. Chang and S.I. Sandler, Mol. Phys. **81**, 745 (1994).
[11] D.A. Young and D.J. Alder, J. Chem. Phys. **73**, 2430 (1980).
[12] C.F. Tejero, A. Daanoun, H.N.W. Lekkerkerker, and M. Baus, Phys. Rev. Lett. **73**, 752 (1994).
[13] R.J. Baxter, J. Chem. Phys. **49**, 2270 (1968).
[14] See, e.g., D. Frenkel, in *Molecular Dynamics Simulation of Statistical Mechanical Systems*, edited by G. Ciccotti and W.G. Hoover (North-Holland, Amsterdam, 1986), p. 151.
[15] R. Hall, J. Chem. Phys. **57**, 2252 (1972).
[16] B.J. Alder, W.G. Hoover, and D.A. Young, J. Chem. Phys. **49**, 3688 (1968).
[17] In fact, the difference in free energy of the face-centered-cubic and hexagonal-close-packed (hcp) structures is so small that it is not known which one is the more stable. Our calculations were performed for the fcc structure, but the results would have been virtually the same for the hcp structure. Other crystal structures (e.g., simple-cubic and body-centered-cubic) can be safely ignored because they have a much lower maximum packing density.
[18] N.F. Carnahan and K.E. Starling, J. Chem. Phys. **51**, 419 (1969).
[19] W.G. Hoover and F.H. Ree, J. Chem. Phys. **49**, 3609 (1968).
[20] D. Frenkel and A.J.C. Ladd, J. Chem. Phys. **81**, 3188 (1984).
[21] W.G Rudd, Z.W. Salzburg, A.P. Yu, and F.H. Stillinger,

J. Chem. Phys. **49**, 4857 (1968).
[22] B. Barboy, J. Chem. Phys. **61**, 3194 (1974).
[23] S.J. Smithline and A.D.J. Haymet, J. Chem. Phys. **83**, 4103 (1985).
[24] C. Cerjan and B. Bagchi, Phys. Rev. A **31**, 1647 (1985).
[25] N.A. Seaton and E.D. Glandt, J. Chem. Phys. **87**, 1785 (1987).
[26] W.G.T. Kranendonk and D. Frenkel, Mol. Phys. **64**, 403 (1988).
[27] G. Stell, J. Stat. Phys. **63**, 1203 (1991).
[28] H. Eyring, J. Chem. Phys. **4**, 238 (1936).
[29] J.E. Lennard-Jones and A.F. Devonshire, Proc. R. Soc. London Ser. A **169**, 317 (1939); **170**, 464 (1939).
[30] J.A. Barker, *Lattice Theories of the Liquid State* (Pergamon, Oxford, 1963).
[31] J.A. Barker, J. Chem. Phys. **44**, 4212 (1966).
[32] A. Daanoun, C.F. Tejero, and M. Baus (unpublished).
[33] C.N. Likos, Zs. T. Németh, and H. Löwen (unpublished).
[34] M.H.J. Hagen and D. Frenkel, J. Chem. Phys. **101**, 4093 (1994).
[35] A. Jayaraman, Phys. Rev. **137**, A179 (1965).
[36] G. Stell and P.C Hemmer, J. Chem. Phys. **56**, 4274 (1972).
[37] B. Alder and D. Young, J. Chem. Phys. **70**, 473 (1979).

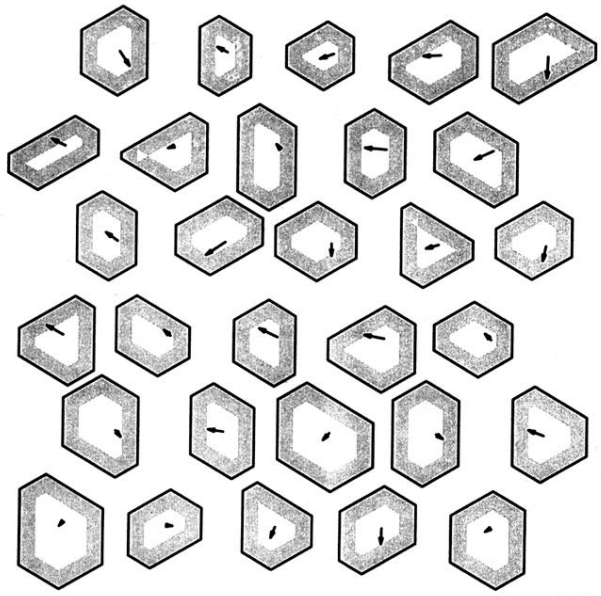

FIG. 4. Schematically drawn scaled configuration of the (2D) square-well solid in the limit $\delta/\sigma \to 0$. The lines of the hexagons give the momentary boundary of the cell to which a particle is confined. All the cell are scaled up to finite size, as the cells are infinitely small in the limit $\delta/\sigma \to 0$. The cell boundaries will change position if the nearest neighbors move. The arrows give the particle displacement from their original lattice positions. In the shaded area the particles are within the interaction range of their neighbors.